

# RELIABILITY-BASED CALENDRIC INSPECTION SCHEDULE FOR AIRCRAFT STRUCTURES WITH CORROSION FATIGUE

Bintuan Wang\* and Seiichi Ito\*\*

\*Japan Society for the Promotion of Science Fellow

\*\* Structures and Materials Research Center, National Aerospace Laboratory of Japan  
6-13-1 Osawa, Mitaka, Tokyo 181-0015 Japan

**Keywords:** *Airframe, Reliability, Bayesian analysis, Corrosion fatigue*

## Abstract

*A Bayesian reliability analysis is applied to determine the optimal non-periodic inspection schedule and estimate the uncertain parameters from field information collected during in-service inspections for aircraft structures with corrosion impact. The procedure is illustrated through typical fuselage structures with number of fatigue critical elements. Assumed, but realistic, probability distribution function for the underlying random variables are used. Monte Carlo simulations are adopted to demonstrate the validity of the analysis.*

*The numerical simulation results show that for case of corrosion, with the same detection capability the first inspection time and the intervals between the subsequent inspection are obviously shorter than that for case of no-corrosion. Structures with more frequent daily flight requires much shorter inspection intervals to sustain their reliability level.*

*It is recognized that the requirement for damage detection and inspection need to be more stringent for structures with corrosion impact.*

## 1 Introduction

Corrosive environment is recognized as significant aspect that affect the reliability, durability and integrity of aircraft. A quantitative approach for defining suitable inspection schedule and mandating repairs is needed for an effective management of an aging fleet of aircraft or new airframe structures serve

in corrosive environment.

Because many uncertain parameters are concerned with reliability analysis of structures and the fact that it is impossible to obtain sufficient actual structural operation data in the present state, an approach for non-periodic inspection by Bayesian method has been developed by Deodatis[1] and Ito[2,3]. However, application of this approach to structures with corrosion impact has not been attempted, and is the principal investigation of this paper. The analysis procedure is performed by two steps: failure process simulation with true structural element model(step I), Bayesian analysis for inspection schedule of the entire structure model(step II). The influences of flight frequency and crack detection capability are also examined in this paper.

The key aspects of References[1,2,3]are repeated as following for completeness.

## 2 Non-periodic inspection by Bayesian method

### 2.1 Model for fuselage structure

#### Structural element model and loading

The fatigue critical element model in this analysis is shown Fig.1. This element in fuselage structures is designed as a 2-bay structure with a skin and three frames.

The primary loading for a commercial aircraft fuselage may be the pressurization-depressurization cycling(Ground-Air-Ground). Thus, the structural element is subjected to a

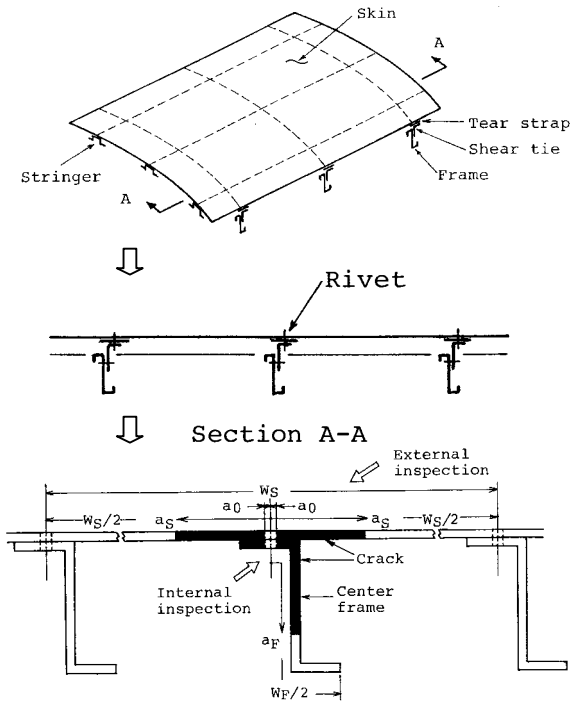


Fig.1. Fatigue critical element of fuselage structure

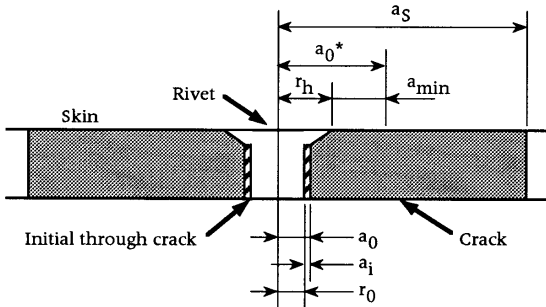


Fig.2. Model of rivet hole and crack

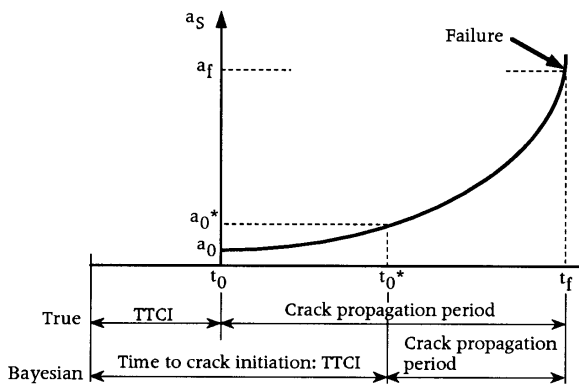


Fig.3. Fatigue crack initiation and propagation for true model and Bayesian analysis

cyclic constant stress range due to GAG loading.

Fatigue crack initiation and propagation

For a specified initiation crack size, the time to crack initiation (TTCI)  $t_0$  is generated by a two-parameter Weibull distribution density function:

$$f(t_0) = \frac{\alpha}{\beta} \left(\frac{t_0}{\beta}\right)^{\alpha-1} \exp\left[-\left(\frac{t_0}{\beta}\right)^\alpha\right] \quad (1)$$

Fatigue cracks growth is calculated from the Paris equation with the stress intensity factor range modified by the following coefficients:

$$\frac{da_s}{dt} = C_s (\Delta K_s)^{b_s} ;$$

$$C_s = 10^{z_s} ; \Delta K_s = \Delta S \sqrt{\pi a_s} \beta_{Frame} \beta_{Bulge} \quad (2)$$

$$\frac{da_F}{dt} = C_F (\Delta K_F)^{b_F} ;$$

$$C_F = 10^{z_F} \quad \Delta K_F = \Delta S \sqrt{\pi a_F} \beta_{WF} \beta_{Skin} \quad (3)$$

where  $\beta_{WF}$  and  $\beta_{Skin}$  denote the effect of finite panel width and the effect of skin crack length respectively.  $\beta_{Frame}$  and  $\beta_{Bulge}$  are the modification for the rupture of frame and the bulge effect of internal pressurization.

Residual strength and element failure criterion

An element can fail either before or after crack initiation. Before crack initiation, the element is considered to have failed when the stress due to flight load exceeds the strength of the element. After crack initiation, the following two modes are considered. One is that a failure due to unstable crack growth occurs when the crack reaches a critical length that is governed by a failure criterion, and the other is that a failure occurs when a crack reaches the 2-bay crack length.

**2.2 Model for Bayesian analysis**

Inspection and probability of detection(PoD)

Detection method I: External visual inspection PoDI has the following form:

$$D_1(a_s^*|d) = 1 - \exp\left[-\left(\frac{a_s^* - a_{min}^{(1)}}{d - a_{min}^{(1)}}\right)^\epsilon\right] \quad (4)$$

Detection method II: Eddy current detection PoDII has the following form[4]

$$D_2(a_s^*) = \{1 + \exp[-\frac{\pi}{\sqrt{3s_0}}(\ln \frac{a_s^* - a_{\min}^{(2)}}{m_0})]\}^{-1} \quad (5)$$

in Eq.(4) and Eq.(5),  $a_s^* = a_s - r_h$ , the minimum detectable crack length is shown in Fig.1. It is assumed that crack in the skin is always symmetric with respect to the central rivet axis. Thus, PoD has the following form:

$$D_i(a_s^*|d) = 1 - [1 - D(a_s^*|d)]^2 \quad (6)$$

If skin crack or failure in a element is detected, repair or replacement is performed and the element is back to its initial state.

#### Fatigue crack initiation and propagation

*TTCI* for initiation crack length  $a_0^* = r_h + a_{\min}$  (Fig.2, Fig.3) has the following form:

$$f^*(t_0^*|\beta^*) = \frac{\alpha}{\beta^*} (\frac{t_0^*}{\beta^*})^{\alpha-1} \exp[-(\frac{t_0^*}{\beta^*})^\alpha] \quad (7)$$

Skin crack propagation rate is assumed to has following form:

$$\frac{da_s}{dt} = C(a_s)^{b/2}; \quad C = 10^z \quad (8)$$

#### Failure rate

The failure rate at time instant  $t$  before crack initiation is given a small constant  $h_0$ . After crack initiation a two-parameter Weibull distribution is adopted for failure rate.

$$h(t) = \exp(r) = h_0 \quad (9)$$

$$h(t) = \frac{\alpha_f}{\beta_f} (\frac{t}{\beta_f})^{\alpha_f-1} + h_0 \quad (10)$$

### 2.3 Bayesian reliability analysis

#### Estimation of the uncertain parameters

The posterior 2-dimensional joint probability density of two uncertain parameters( $\beta^*, z$ ) after the  $j$ -th inspection is given by the following equation:

$$f^j(\beta^*, z) = \frac{LF_j \cdot f^0(\beta^*, z)}{\int_{\beta_{\min}^*}^{\beta_{\max}^*} \int_{z_{\min}}^{z_{\max}} (Numerator) d\beta^* dz} \quad (11)$$

where  $LF_j$  denotes the likelihood function for the entire structures consisting of  $M$  fatigue critical elements as a result of the  $j$ -th inspection. All of the elements are inspected at every inspection, the initial prior 2-dimensional joint  $j=0$ , of the two parameters is chosen to be uniformly distributed.

#### Computation of time for the next inspection $T_{j+1}$

The reliability of entire structure at the time instance  $t^*$  after the latest inspection  $T_j$  is computed by the following equation:

$$R_M(t^*) = \int_{\beta_{\min}^*}^{\beta_{\max}^*} \int_{z_{\min}}^{z_{\max}} R_M(t^*|\beta^*, z) \cdot f^j(\beta^*, z) d\beta^* dz \quad (12)$$

As the entire structure must maintain its reliability above a prespecified level throughout its service life, the next inspection time  $T_{j+1}$  after the latest one performed at  $T_j$  is calculated by:

$$R_M(t^*) \geq R_{design}; T_{j+1} = t^* = \bar{R}_M^{-1}(R_{design}) \quad (13)$$

where  $R_{design}$  denotes the prespecified design level of reliability.

### 3 Selection of variables for Corrosion fatigue

For simplification of analysis, it is assumed here that the entire structure exposes to corrosion environment from the time of service initiation. Each element is defined so that it possesses only one corrosion fatigue critical location where a dominative corrosion origin can grow into a through-the thickness crack, and the crack propagate into a critical length governed by failure criterion. Thus, for aluminum alloy(2024-T3 and 7075-T6), the variables for corrosion fatigue initiation and growth can be estimated as follow.

#### 3.1 Parameters for *TTCI*

##### Fixed flight frequency

Time to crack initiation(*TTCI*) is assumed to follow two-parameter Weibull distribution, the statistical characteristics for case of corrosion and no-corrosion are assumed:

$$\mu_{TTCI_{cor.}} = 1/5 \mu_{TTCI_{no-cor.}}$$

$$COV_{TTCI_{cor.}} = 70\% COV_{TTCI_{no-cor.}}$$

$\mu_{TTCI_{cor.}}$  and  $COV_{TTCI_{cor.}}$  denote mean and coefficient of variation(COV) for case of corrosion respectively.  $\mu_{TTCI_{no-cor.}}$  and  $COV_{TTCI_{no-cor.}}$  for case of no-corrosion.

Such values of proportion are based on some predicted results for 2024-T3 unclad plate with a open hole: the mean of pit corrosion fatigue crack initiation life for a nucleated pit(mean size 0.005mm) to grow into a through thickness crack(1.27mm) is about 20% of that without pitting corrosion[4].

Another evidence is: the average fatigue life of the prior pitting corrosion specimens(3.5%NaCl aerated aqueous solution and an applied electrical supply). was decreased by a factor of 6.5-10.2 when compared to that of no-corrosion environment[5].

The ratio of COV between corrosion and no-corrosion is from a pre-corrosion fatigue test results for 2024-T3 splice specimens[6].

#### Different flight frequency

According to fatigue damage rule,  $TTCI$  is proportional reversely to flight frequency. For example, when flight frequency increases from 2cyc/day to 10cyc/day,  $TTCI$  can decrease to 1/5 of that for 2cyc/day. But for case of corrosion, the proportion can be 1/3 [7], because the time for a pit to grow into a surface crack depends on pitting corrosion model.

### 3.2 Corrosion fatigue crack propagation

The coefficient of crack propagation rate is assumed to follow Normal distribution, and the statistical characteristics for case of corrosion and no-corrosion are assumed:

$$\mu_{C_{cor.}} = 3\mu_{C_{no-cor.}}; COV_{C_{cor.}} = 110\% COV_{C_{no-cor.}}$$

$$b_{cor.} = b_{no-cor.}$$

$\mu_{C_{cor.}}$  and  $COV_{C_{cor.}}$  denote mean and coefficient of variation for case of corrosion respectively.  $\mu_{C_{no-cor.}}$  and  $COV_{C_{no-cor.}}$  for case of no-corrosion.

The ratio of mean is based on a estimated results of 2024-T3 alloy for air and 0.5M NaCl solution [8] and the physics nature of crack

propagation: the coefficient  $C$  characterizes the variability in the material property including microstructural and environmental parameters, but the exponent  $b$  represents the mechanistic dependence of the crack growth rate on the driving force  $\Delta K$ . The ratio of COV is also estimated from experimental results[6].

### 3.3 Failure rate

The parameters  $\alpha_f$  and  $\beta_f$  is estimated by two steps: Step I-Simulate the failure process and calculate the fatigue crack propagation life with Monte Carlo method, Step II-Estimate the failure rate function.

### 4 Numerical example

The computation is performed with two steps. In the first step failure process is simulated with true mode to get information of a specific inspection. In the second step, the simulated results are used to determine the inspection time, and two parameters  $\beta, z$  and are considered to be uncertain. A brief explanation for parameters selection is as following section.

Three cases are considered:

Case1: No-corrosion, flight frequency 2cyc/day, two levels of detection capability PoDI(d=1.2, 0.4);

Case2: With corrosion, flight frequency 2cyc/day, two levels of detection capability PoDI(d=1.2, 0.4);

Case3: With corrosion, flight frequency 10cyc/day, three levels of detection capability PoDI(d=1.2, 0.4) and PoDII.

### 4.1 Parameters values for first step

#### Materials

2024-T3 and 7075-T6 are selected for skin and frame respectively.

#### Strength and fracture toughness

Both strength and fracture toughness are assumed to follow two-parameter Weibull distribution, and the parameters are estimated based on MILL-HDBK-5F and Damage

Tab. 1. Values of parameters in numerical example

Item	Case1(PoDI-A,C)		Case2(PoDI-A,C)		Case3(PoDI-B,C; PoDII)	
	True model	Bayesian analysis	True model	Bayesian analysis	True model	Bayesian analysis
Service life(days)	20000		5000		1600	
Total Num. of elements: $M$	50		50		50	
Rivet head radius: $r_h$ (in)	0.18		0.18		0.18	
Initial half crack length(in) for true model: $a_0$ for Bayesian analysis: $a_0^*$	0.168		0.168		0.168	
Effective width: Skin: $W_S$ Frame: $W_{F1}, W_{F2}$	40 14, 2		40 14, 2		40 14, 2	
Max.allowable crack length(in) Skin: $a_{S,max}$ Frame: $a_{F1,max}, a_{F2,max}$	20 7, 1		20 7, 1		20 7, 1	
Yield stress $S_y$ (ksi) 2-parameter Weibull $\alpha_{S_y}$ $\beta_{S_y}$	Skin 2024 19 49	Frame 7075 19 70	Skin 2024 19 49	Frame 7075 19 70	Skin 2024 19 49	Frame 7075 19 70
Fracture toughness $K_{Ic}$ (ksi√in) 2-parameter Weibull $\alpha_{K_{Ic}}$ $\beta_{K_{Ic}}$	12 140	12 65	12 140	12 65	12 140	12 65
Cyclic stress range: $\Delta S$ (ksi) Normal $\mu_{\Delta S}$ $\sigma_{\Delta S}$	18 0.9	18 0.9	18 0.9	18 0.9	18 0.9	18 0.9
Parameters of PoDI: $\epsilon, a_{min}^{(1)}$ $d$ PoDII: $m_0, s_0, a_{min}^{(2)}$	1.4, 0.04 1.2(A), 0.4(C)		1.4, 0.04 1.2(A), 0.4(C)		1.4, 0.04 0.8(B), 0.4(C) 0.05, 0.572, 0	
Parameters of $TTCI$ (days) 2-parameter Weibull $\alpha$ $\beta$	4 20000	4 (11000~33000)	5.95 3910	5.95 (2900~6000)	5.95 1303	5.95 (900~2000)
Crack propagation Normal $b$ $\mu_z$ $\sigma_z$ $z$	3.9 -9.4 0.183	3.5 -8.4 0.183	3.9 -8.92 0.193	3.5 -7.92 0.190	3.9 -8.22 0.193	3.5 -7.22 0.190
Failure rate: $r, \alpha_f, \beta_f$ (days)	-17.3, 2.57, 8919		-15.7, 2.46, 3047		-14.1, 2.52, 605	

Tolerant Design HDBK. Since no evidence reported on different  $S_y$  or  $K_{Ic}$  between corrosion environment and no-corrosion environment, the same values are selected for case of corrosion condition.

TTCI

$\alpha$  and  $\beta$  are selected to be 4 and 20000days(for 2cyc/day) for no-corrosion condition. For corrosion condition, with two kinds of flight frequency, the parameters are selected according to the advised requirements mentioned in 3.1.

Crack propagation

In Eq.(8),two variables  $C$  and  $b$  are assumed to be normal distribution, they are selected from the typical values for aluminum alloy. The parameters for corrosion condition are determined from 3.2.

Failure rate

When the determined and random parameters are selected for all cases, the parameters  $\alpha_f$  and  $\beta_f$  in failure rate functions Eq.(10)can be estimated by approach mentioned in 3.3.

4.2 Parameters values for second step

Uncertain parameters

$\beta^*$  in Eq.(7) and  $z$  in Eq.(8) are considered as uncertain and needed to be estimated, their range are given in Tab1.

Service life

The aircraft is assumed to have 50 fatigue critical elements The service life of the structures are 20000days,5000days,1600days for no-corrosion ( $f=2cyc/day$ ), corrosion ( $f=2, 10cyc/day$ ) respectively. The purpose on selection of shorter service life for corrosion case is attributed to shorter  $TTCI$ . for corrosion case. The reliability level required for entire structure is 0.8.

Probability of crack detection

For PoDI, selections of  $d=1.2,0.8,0.4$  aims to investigate the effect of different PoD on inspection.  $d=1.2$  denotes lower PoD. Compared with PoDI, PoDII for same crack size is nearly 100 times higher capability. For example, PoD for a crack size of 0.05inch are

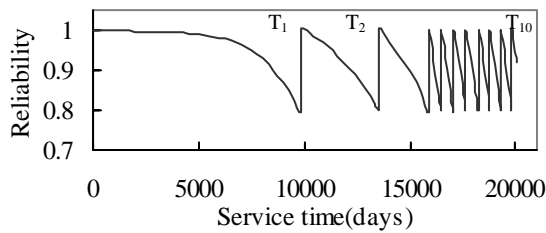


Fig.4. Inspection schedule and structural reliability (Case 1, PoDI, d=1.2)

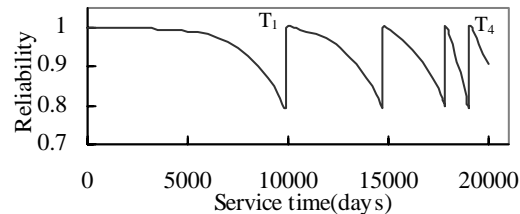


Fig.5. Inspection schedule and structural reliability (Case 1, PoDI, d=0.4)

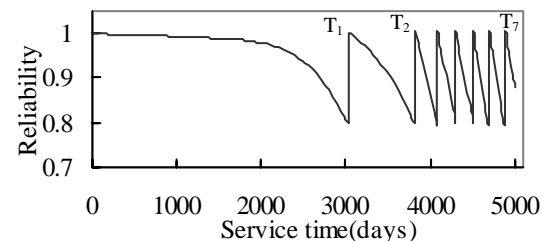


Fig.6. Inspection schedule and structural reliability (Case 2, PoDI, d=1.2)

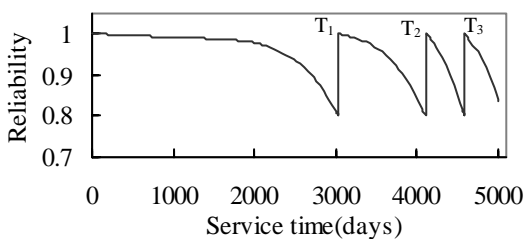


Fig.7. Inspection schedule and structural reliability (Case 2, PoDI, d=0.4)

0.13%, 0.67%, 50% for PODI (d=1.2, 0.4), and PODII respectively. Values of parameters are listed in Tab.1

### 4.3 Computational results

With above procedure and parameters, the computation is implemented, some results are shown in Tab.2 (A, B, C note PoDI for d=1.2, 0.8, 0.4 respectively), and Fig.4~Fig.20, that show:

#### Non-experiodic inspection intervals

Non-periodically inspection intervals for both cases of corrosion and no-corrosion are generated.

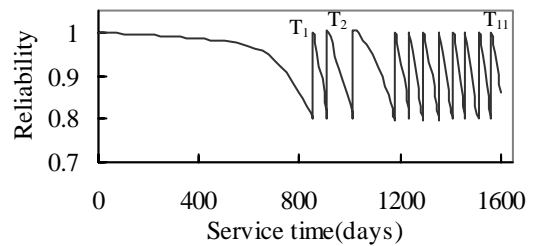


Fig.8. Inspection schedule and structural reliability (Case 3, PoDI, d=0.8)

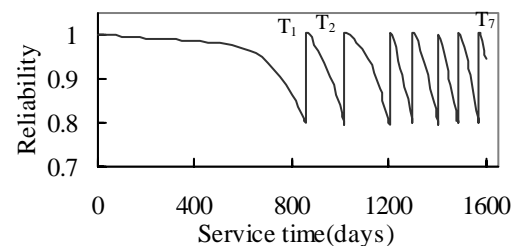


Fig.9. Inspection schedule and structural reliability (Case 3, PoDI, d=0.4)

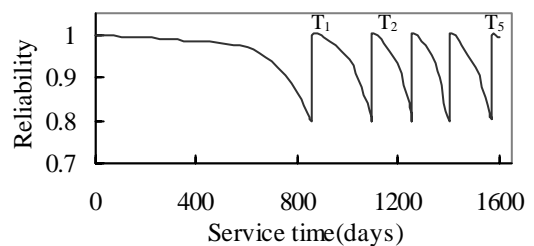


Fig.10. Inspection schedule and structural reliability (Case 3, PoDI, d=0.4)

#### Shorter inspection interval for corrosion case

The inspection intervals for case of corrosion are obviously shorter than that for no-corrosion. For the same flight frequency and same detection level (PoDI, d=1.2), Comparison between Case 1 and Case 2 (Tab.2, Fig.4~7) shows: the first inspection time for corrosion (3026 days) is only 1/3 of that for no-corrosion (9860 days). The ratio for second interval is about 1/5; after the third inspection, the ratio of average interval is 1/3.

These results imply that for case of corrosion if the inspection schedule were performed same as that for no-corrosion, the corroded structures would not sustain their required reliability level. Actually, even before first inspection (9860 days), most corroded elements would fail (simulated results show 10 corroded elements can fail till 5000 days service). Obviously, performing a much frequent inspection schedule is necessary.

Tab.2. Results for three cases

Inspection No.	Inspection time(days)							Number of failed elements						Number of detected cracks							
	Case1		Case2		Case3			Case1		Case2		Case3		Case1		Case2		Case3			
	A	C	A	C	PoDI	PoDI	PoDI	A	C	A	C	PoDI	PoDI	A	C	A	C	PoDI	PoDI		
1	9860	9860	3026	3026	855	855	855	0	0	0	0	2a, 1b	2a, 1b	2a, 1b	0	0	0	0	0	0	1
2	13510	14660	3811	4115	910	1016	1095	0	1a	1a	1a	0	0	0	1	1	1	8	0	2	12
3	15910	17800	4087	4593	1015	1204	1255	1a	3a	0	0	0	1a	0	3	9	4	4	1	5	14
4	16470	19020	4296		1182	1295	1404	0	0	0		1a	0	2	5	3		4	6	11	
5	17060		4511		1237	1403	1568	0		1a		0	1a	0	2		1		2	7	8
6	17630		4695		1294	1481		0		0		0	0	2		1		5	3		
7	18210		4883		1353	1569		0		0		1a	0	2		4		1	2		
8	18760				1408			1a				0		2				3			
9	19260				1460			0				0		4				2			
10	19780				1512			0				0		1				5			
11					1563							0						3			

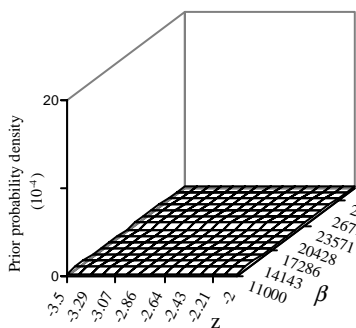


Fig.11. Prior joint density (Case1,PoDI,d=1.2)

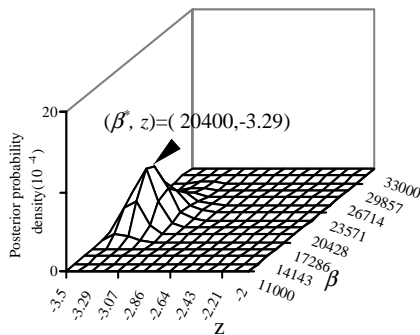


Fig.12. Posterior joint density at 4th inspection(Case1,PoDI,d=1.2)

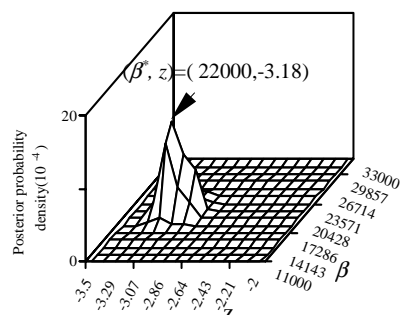


Fig.13. Posterior joint density at 4th inspection(Case1,PoDI,d=0.4)

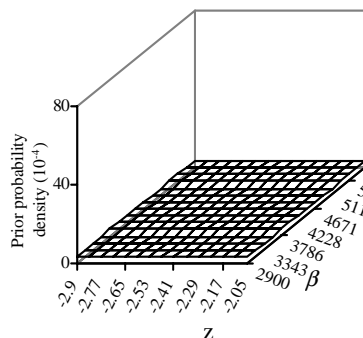


Fig.14. Prior joint density (Case2,PoDI,d=1.2)

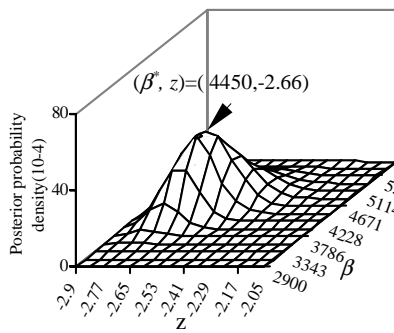


Fig.15. Posterior joint density at 3rd inspection(Case2,PoDI,d=1.2)

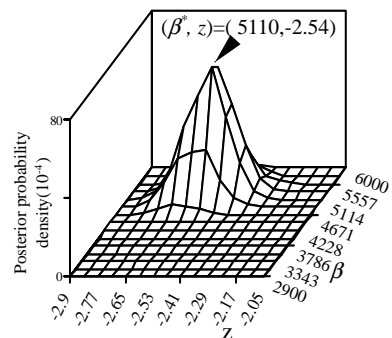


Fig.16. Posterior joint density at 3rd inspection(Case2,PoDI,d=0.4)

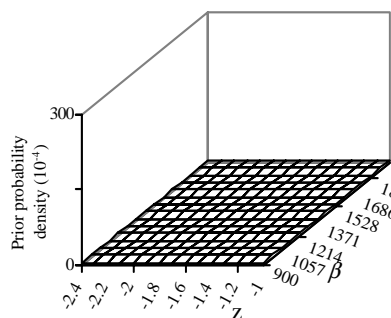


Fig.17. Prior joint density (Case3,PoDI,d=0.8)

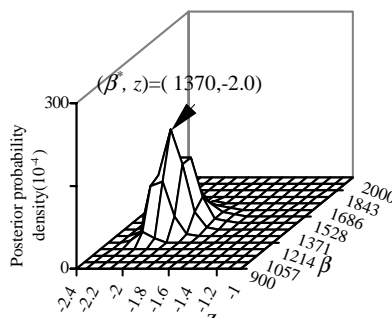


Fig.18. Posterior joint density at 5th inspection(Case3,PoDI,d=0.8)

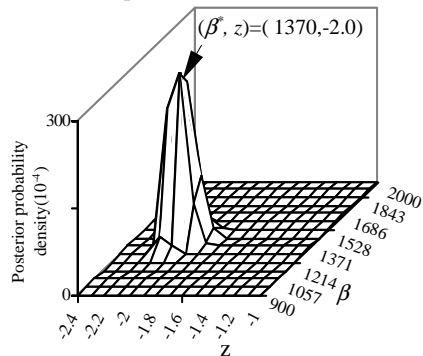


Fig.19. Posterior joint density at 5th inspection(Case3,PoDI,d=0.4)

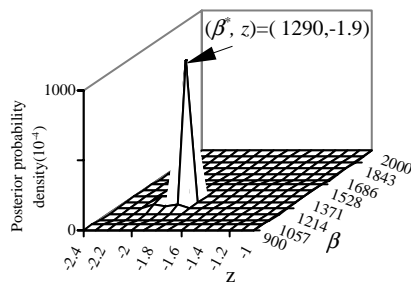


Fig.20. Posterior joint density at 5th inspection(Case3,PoDII)

### Effect of flight frequency

For case of corrosion, with the same detection level (PoDI,  $d=0.4$ ), the results in Fig.7 and Fig.9 show: the inspection intervals for short haul (10cyc/day) is also shorter compared with that of long haul (2cyc/day). The first inspection for the former (855 days) is only 28% of that for the later (3026 days). The ratio for the second and third inspection intervals are 15% and 39% respectively. After the third inspection, the average intervals for  $f=10$  cyc/days is only 90 days.

### Effect of PoD

The higher capability of PoD is used, the less total inspection times is required, that can be easily found in Tab.1 and Fig.4~Fig.10.

Another aspect is that with same inspection times the number of cracks as well as those with smaller size detected by higher PoD level is obvious with priority. Take Case3 as example, for three PoD levels - PoDI ( $d=0.8, d=0.4$ ) and PoDII, in the second inspection, the number of detected cracks are 0, 2 and 12 respectively. The total number of cracks (also the number of elements with crack in the 50 elements) till second inspection are 6, 9, 13. That shows the benefit of PoDII is striking. For structures with corrosion, higher PoD is particularly important, that directly determines the cost of repair. Generally a crack size 0.05 inch is considered as the economical repair limit for a crack initiated from a rivet hole. Because of the earlier crack initiation and higher crack propagation rate for structural elements with corrosion, the reliability of structure can decline much quickly. Thus, a high PoD for crack size smaller than 0.05 inch is benefit to engineering

repair.

### Posterior probability density (PPD) of uncertain parameters

The posterior joint probability density of the uncertain parameters  $(\beta^*, z)$  for three Cases are plotted in Fig.11~Fig.20. Unimodal aspects appear in the posterior density for all Cases after 3<sup>rd</sup> inspection. The effect of PoD is also observed, that is, with higher PoD, the unimodal density is also higher after same number of inspection. For instance, Max. PPD in Fig.13 (Fig.16) is 1.6 times as large as that in Fig.12 (Fig.15). Max. PPD in Fig.19 and Fig.20 are 1.6 times and 5.7 times as large as that in Fig.18 respectively.

## 5 Conclusion

A typical commercial transport fuselage structure with fatigue critical elements is used as a realistic model for the present analysis. Each element comprises a skin panel and three frames and is subjected to pressurization-depressurization cycling. The structure is assumed to be exposed to aqueous corrosion environment as well as no-corrosion environment. Undetermined aspects considered are fatigue crack initiation and propagation, failure rate function and crack detection capability.

Monte Carlo method is adopted to demonstrate the validity of the Bayesian reliability analysis. As a result, the optimum non-periodic calendric inspection schedule is implemented. Also, the uncertain parameters are estimated using the information gathered during the inspection.

For case of corrosion, with the same detection capability the first inspection time and the intervals between the subsequent inspection are obviously shorter than that for case of no-corrosion. Structure with more frequent daily flight requires much shorter inspection intervals to sustain their reliability level. However, less inspection times is needed with aid of higher crack detection capacity.

Due to earlier crack initiation and higher crack propagation rate for structural elements with corrosion, however, the requirements for



damage detection and inspection should be more stringent.

It should be mentioned in this numerical example, that the selection of parameters values for corrosion model is somewhat arbitrary that refers to insufficient data, but the analytical results remain qualitatively practical. In reality, aircraft structures (including rivet holes) are protected quite well; however, when they have been compromised by corrosion, corrective action such as repair becomes urgent.

### Acknowledgements

This research is supported by Japan Society for the Promotion of Science under Fellowship and Full-Scale Testing Group, Structures and Materials Research Center of National Aerospace Laboratory of Japan.

### Reference

- [1] Deodatis,G.,et al. Non-periodic inspection by Bayesian method I. *Probability Engineering Mechanics*, Vol.7, No.4, pp191-204, 1992.
- [2] Ito,Seiichi.,et al. Non-periodic inspection by Bayesian method II:Structures with elements subjected to different stress levels. *Probability Engineering Mechanics*, Vol.7, No.4, pp205-215, 1992.
- [3] Ito,Seiichi.,et al. Reliability analysis of pressurized fuselage structure. *Proceeding of The 37<sup>th</sup> Structures Conference of Japan Society of Aeronautical and Space Science*,Tokyo,Japan,1B44, pp121-124,1995.
- [4] Harlow,D.G. and Wei,R.P. Probability of occurrence and detection of damage in airframe materials. *Fatigue Fract .Engng Mater. Struct.* Vol.22, pp427-436,1999.
- [5] Clark,Paul N. and Hoepfner,David W. Corrosion pitting and the transition to surface fatigue cracks in 2024-T3 aluminum alloy. *The 21<sup>st</sup> Symposium of the International Committee on Aeronautical Fatigue*,Toulouse,France, 2001.
- [6] Liao,M. and Xiong,Y. Risk analysis of fuselage splices containing multisite damage and corrosion. *Journal of Aircraft*, Vol.38, No.1, pp181-187,2001.
- [7] Harlow,D.G. and Wei,R.P. Probability approach for prediction of corrosion and corrosion fatigue life. *AIAA JOURNAL*, Vol.32, No.10, pp2073-2079,1994.
- [8] Wei,R.P. et al. Probability modeling of corrosion fatigue crack growth and pitting corrosion. *Proceeding of the25th International Conference on Aeronautical Fatigue*,Edinburgh,U.K., 1997.